Liquid-Phase Patterning and Microstructure of Anatase TiO_2 Films on SnO_2:F Substrates Using Superhydrophilic Surface†

Yoshitake Masuda* and Kazumi Kato

National Institute of Advanced Industrial Science and Technology (AIST), 2266-98 Anagahora, Shimoshidami, Moriyama-ku, Nagoya 463-8560, Japan

Received April 15, 2007. Revised Manuscript Received June 11, 2007

Liquid-phase patterning of crystalline anatase TiO_2 thin films on SnO_2:F substrates was successfully achieved using a superhydrophilic surface. The superhydrophilic surface on the SnO_2:F substrate was micropatterned by UV irradiation (184.9 and 253.7 nm) through a photomask. The substrate was then immersed in an aqueous solution containing ammonium hexafluorotitanate and boric acid at 50 °C. Anatase TiO_2 crystallized to form thin films on the superhydrophilic regions selectively because of the acceleration of nucleation and crystal growth. A micropattern of anatase TiO_2 was thus fabricated on a SnO_2:F substrate in the aqueous solution without any insulating layers, which decrease electrical conductivity between the TiO_2 film and SnO_2:F substrate. The micropattern was constructed of anatase TiO_2 film, in which an assembly of nano TiO_2 crystals covered the surface.

1. Introduction

Titanium dioxide (TiO_2) thin films have been widely exploited in many applications such as microelectronics,[1] optical cells,[2] solar energy conversion,[3] highly efficient catalysts,[4] microorganism photolysis,[5] antifogging and self-cleaning coatings,[6] gratings,[7] gate oxides in metal-oxide-semiconductor field-effect transistors (MOSFET),[8,9] etc. Accordingly, various attempts have been made to fabricate thin films and micropatterns of TiO_2 by several methods, and in particular, to synthesize materials and devices including TiO_2 thin films from an aqueous solution through an environmentally friendly synthesis process, i.e., "green chemistry".

TiO_2 films have been prepared from aqueous solutions via various methods.[10–20] Deki et al.[10–13] prepared amorphous TiO_2 thin films on glass substrates at 30 °C from $(NH_4)_2TiF_6$ aqueous solution using liquid-phase deposition, which was first used for SiO_2.[21] Recently, liquid-phase crystal deposition (LPCD) was successfully used to fabricate crystalline anatase TiO_2 in an aqueous solution at 50 °C,[22] allowing crystalline anatase TiO_2 to be prepared without high-temperature annealing. Additionally, nano/micropatterns of their films were fabricated using self-assembled monolayers (SAMs) on substrates.[23,24] Molecular recognition and organic−inorganic interactions between SAMs and TiO_2 were used for the liquid-phase patterning. These processes have paved the way for the fabrication of next-generation green devices. Nano/micropatterns of various oxides[25–37] and colloidal crystals[38–42] have been demonstrated for electric devices, optical devices, and solar cells. However, the patterning processes require the use of self-assembled monolayers as templates, which restricts their scope of application. Additionally, the organic monolayer remains under the oxide

† Part of the "Templated Materials Special Issue".

* Corresponding author. E-mail: masuda-y@aist.go.jp.

(1) Burns, G. P. *J. Appl. Phys.* **1989**, *65*, 2095–2097.
(2) Yoldas, B. E.; O'Keeffe, T. W. *Appl. Opt.* **1979**, *18* (18), 3133–3138.
(3) Butler, M. A.; Ginley, D. S. *J. Mater. Sci.* **1980**, *15* (1), 1–19.
(4) Carlson, T.; Giffin, G. L. *J. Phys. Chem.* **1986**, *90* (22), 5896–5900.
(5) Matsunaga, T.; Tomoda, R.; Nakajima, T.; Nakamura, N.; Komine, T. *Appl. Environ. Microbiol.* **1988**, *54* (6), 1330–1333.
(6) Wang, R.; Hashimoto, K.; Fujishima, A. *Nature* **1997**, *388* (6641), 431–432.
(7) Borenstain, S. I.; Arad, U.; Lyubina, I.; Segal, A.; Warschawer, Y. *Thin Solid Films* **1999**, *75* (17), 2659–2661.
(8) Peercy, P. S. *Nature* **2000**, *406* (6799), 1023–1026.
(9) Wang, D. J.; Masuda, Y.; Seo, W. S.; Koumoto, K. *Key Eng. Mater.* **2002**, *214* (2), 163–168.
(10) Deki, S.; Aoi, Y.; Hiroi, O.; Kajinami, A. *Chem. Lett.* **1996**, *6*, 433–434.
(11) Deki, S.; Aoi, Y.; Yanagimoto, H.; Ishii, K.; Akamatsu, K.; Mizuhata, M.; Kajinami, A. *J. Mater. Chem.* **1996**, *6* (12), 1879–1882.
(12) Deki, S.; Aoi, Y.; Asaoka, Y.; Kajinami, A.; Mizuhata, M. *J. Mater. Chem.* **1997**, *7* (5), 733–736.
(13) Kishimoto, H.; Takahama, K.; Hashimoto, N.; Aoi, Y.; Deki, S. *J. Mater. Chem.* **1998**, *8* (9), 2019–2024.
(14) Chen, Q.; Qian, Y.; Chen, Z.; Jia, Y.; Zhou, G.; Li, X.; Zhang, Y. *Phys. Status Solidi A* **1996**, *156* (2), 381–385.
(15) Huang, D.; Xiao, Z.-D.; Gu, J.-H.; Huang, N.-P.; Yuan, C.-W. *Thin Solid Films* **1997**, *305* (1–2), 110–115.
(16) Shimizu, K.; Imai, H.; Hirashima, H.; Tsukuma, K. *Thin Solid Films* **1999**, *351* (1–2), 220–224.
(17) Wang, X. P.; Yu, Y.; Hu, X. F.; Gao, L. *Thin Solid Films* **2000**, *371* (1–2), 148–152.
(18) Lee, M. K.; Lei, B. H. *Jpn. J. Appl. Phys.* **2000**, *39* (2A), L101–103.
(19) Selvaraj, U.; Prasadarao, A. V.; Komarneni, S.; Roy, R. *J. Am. Ceram. Soc.* **1992**, *75* (5), 1167–1170.
(20) Niesen, T. P.; DeGuire, M. R. *J. Electroceram.* **2001**, *6* (3), 169–207.
(21) Nagayama, H.; Honda, H.; Kawahara, H. *J. Electrochem. Soc.* **1988**, *135* (8), 2013–2016.
(22) Masuda, Y.; Sugiyama, T.; Seo, W. S.; Koumoto, K. *Chem. Mater.* **2003**, *15* (12), 2469–2476.
(23) Masuda, Y.; Saito, N.; Hoffmann, R. De.; Guire, M. R.; Koumoto, K. *Sci. Technol. Adv. Mater.* **2003**, *4*, 461–467.
(24) Xiang, J. H.; Masuda, Y.; Koumoto, K. *Adv. Mater.* **2004**, *16* (16), 1461–1464.
(25) Aizenberg, J.; Black, A. J.; Whitesides, G. M. *Nature* **1999**, *398*, 495–498.
(26) Aizenberg, J.; Black, A. J.; Whitesides, G. M. *J. Am. Chem. Soc.* **1999**, *121* (18), 4500–4509.
(27) Masuda, Y.; Kinoshita, N.; Sato, F.; Koumoto, K. *Cryst. Growth Des.* **2006**, *6* (1), 75–78.
(28) Nakanishi, T.; Masuda, Y.; Koumoto, K. *Chem. Mater.* **2004**, *16*, 3484–3488.

10.1021/cm071026t CCC: $40.75
Published on Web 08/22/2007

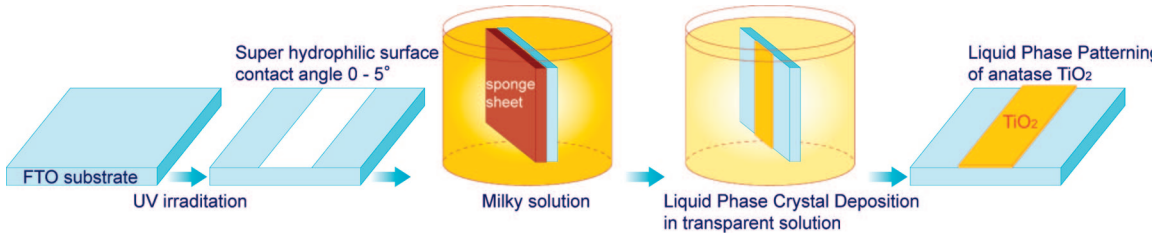

Figure 1. Conceptual process for liquid-phase patterning of anatase TiO_2 films using a superhydrophilic surface.

film, which decreases the electrical conductivity between the oxide film and substrate.

In this study, we achieved liquid-phase patterning (LPP) of crystalline anatase TiO_2 films on SnO_2:F substrates (FTO) using a superhydrophilic surface instead of self-assembled monolayers.[43] The superhydrophilic surface prepared by strong UV irradiation accelerated the nucleation and crystallization of anatase TiO_2, whereas deposition was suppressed on a hydrophobic initial SnO_2:F surface. Anatase TiO_2 was thus deposited only on the superhydrophilic SnO_2:F surface directly to form a micropattern. The micropattern consisted of anatase TiO_2 film in which an assembly of nano TiO_2 crystals covered the surface.

2. Experimental Section

2.1. Micropatterning of Superhydrophilic Surface. A glass substrate coated with a F-doped SnO_2 transparent conductive film (FTO, SnO_2:F, Asahi Glass Co., Ltd., 9.3–9.7 Ω/□, 26 × 50 × 1.1 mm) was blown by air to remove dust and exposed to ultraviolet light (low-pressure mercury lamp PL16−110, air flow, 100 V, 200 W, SEN Lights Co., 14 mW/cm^2 for 184.9 nm at a distance of 10 mm from the lamp, 18 mW/cm^2 for 253.7 nm at a distance of 10 mm from the lamp) for 10 min through a photomask (Test-chart-No.1-N type, quartz substrate, 1.524 mm thickness, Toppan Printing Co., Ltd.) (Figure 1).

2.2. Liquid-Phase Crystal Deposition of Anatase TiO_2. Ammonium hexafluorotitanate ($[NH_4]_2TiF_6$) (Morita Chemical Industries Co., Ltd., FW: 197.95, purity 96.0%) and boric acid (H_3BO_3) (Kishida Chemical Co., Ltd., FW: 61.83, purity 99.5%) were used as received. Ammonium hexafluorotitanate (2.0620 g) and boric acid (1.8642 g) were separately dissolved in deionized water (100 mL) at 50 °C. Boric acid solution was added to ammonium hexafluorotitanate solution at concentrations of 0.15 and 0.05 M, respectively.

The SnO_2:F substrate having a patterned surface with hydrophobic regions and superhydrophilic regions was covered by a silicon rubber sponge sheet (Silico-sheet, SR-SG-S 5mmt RA grade, Shin-etsu Finetech Co., Ltd.) to suppress deposition of TiO_2 at the initial stage. The substrate was immersed perpendicularly in the middle of the solution (Figure 1). The solution was kept at 50 °C with no stirring. The silicon rubber sponge sheet was removed from the SnO_2:F substrate after 25 h, and the substrate was then kept for a further 2 h at 50 °C. The substrate was covered by the sheet instead of immersion of substrate at 25 h to avoid agitation of the solution.

2.3. Characterization. Morphology of TiO_2 was observed by a field-emission scanning electron microscope (FE-SEM; JSM-6335F, JEOL Ltd.) and a transmission electron microscope (TEM; H-9000UHR, 300 kV, Hitachi). Micropattern of thin films was evaluated by SEM and a thick film deposited for 25 h was evaluated by TEM. The crystal phase was evaluated by an X-ray diffractometer (XRD; RINT-2100V, Rigaku) with Cu Kα radiation (40 kV, 30 mA). The diffraction patterns were evaluated using ICSD (Inorganic Crystal Structure Database) data (FIZ Karlsruhe, Germany and NIST,) and FindIt.

Solution condition was evaluated as a function of time without immersion of a substrate. Five vessels containing 200 mL of mixed solution of ammonium hexafluorotitanate and boric acid were prepared to evaluate the solution condition. The supernatant solution of 100 mL was removed from the solution of 200 mL at 0.5, 1, 2, 5, or 25 h from each vessel. The supernatant solution was filtered by a filter paper (Whatman 5, >2.5 μm), a glass filter paper (Whatman GF/B, >1.0 μm) or a filter syringe (Whatman PTFE 0.2, >0.2 μm) in this order. Filters were weighed after drying at 70 °C for 7 days to estimate the weight of solid constituents. Each filter trapped particles of different sizes such as particles >2.5 μm in diameter by the filter paper (Whatman 5), 2.5–1.0 μm in diameter by the glass filter paper (Whatman GF/B), or particles 1.0–0.2 μm in diameter by the filter syringe (Whatman PTFE 0.2). The filtrate that collected in all filters was dried at 70 °C for 7 days to weigh the precipitate. The residual solution of 100 mL after removing the supernatant solution was filtered by the filter paper (Whatman 5, >2.5 μm). The filter paper was weighed after drying at 70 °C for 7 days to estimate the weight of precipitated particles >2.5 μm in diameter.

3. Results and Discussion

3.1. Micropatterned Surface Modification of SnO_2:F Substrate to Superhydrophilic Surface. The initial SnO_2:F substrate showed a water contact angle of 96°. The UV-irradiated surface was, however, wetted completely (contact

(29) Aizenberg, J.; Braun, P. V.; Wiltzius, P. *Phys. Rev. Lett.* **2000**, *84* (13), 2997–3000.
(30) Cho, Y. R.; Lee, J. H.; Song, Y. H.; Kang, S. Y.; Hwang, C. S.; Jung, M. Y.; Kim, D. H.; Lee, S. K.; Uhm, H. S.; Cho, K. I. *Mater. Sci. Eng., B* **2001**, *79* (2), 128–132.
(31) Jeon, N. L.; Clem, P. G.; Nuzzo, R. G.; Payne, D. A. *J. Mater. Res.* **1995**, *10* (12), 2996–2999.
(32) Nashimoto, K.; Haga, K.; Watanabe, M.; Nakamura, S.; Osakabe, E. *Appl. Phys. Lett.* **1999**, *75* (8), 1054–1056.
(33) Mott, M.; Song, J. H.; Evans, J. R. G. *J. Am. Ceram. Soc.* **1999**, *82*, 1653–1658.
(34) Stutzmann, N.; Tervoort, T. A.; Bastiaansen, C. W. M.; Feldman, K.; Smith, P. *Adv. Mater.* **2000**, *12* (8), 557–562.
(35) Bauer, W.; Ritzhaupt-Kleissl, H. J.; Hausselt, J. *Ceram. Int.* **1999**, *25* (3), 201–205.
(36) Jacobs, H. O.; Whitesides, G. M. *Science* **2001**, *291* (5509), 1763–1766.
(37) Kim, C.; Burrows, P. E.; Forrest, S. R. *Science* **2000**, *288* (5467), 831–833.
(38) Masuda, Y.; Itoh, T.; Koumoto, K. *Adv. Mater.* **2005**, *17* (7), 841–845.
(39) Masuda, Y.; Itoh, T.; Koumoto, K. *Langmuir* **2005**, *21*, 4478–4481.
(40) Kim, E.; Xia, Y.; Whitesides, G. M. *Adv. Mater.* **1996**, *8*, 245–247.
(41) Ozin, G. A.; Yang, S. M. *Adv. Func. Mater.* **2001**, *11* (2), 95–104.
(42) Xia, Y. N.; Yin, Y. D.; Lu, Y.; McLellan, J. *Adv. Func. Mater.* **2003**, *13* (12), 907–918.
(43) Masuda, Y.; Kato, K. Nano acicular anatase TiO_2 assembly particle and porous anatase TiO_2 crystal film and method of manufacturing same. Japanese Patent Application Number P2007−100949, April 6, 2007.

angle 0–1°). The contact angle decreased with irradiation time (96, 70, 54, 35, 14, 5, and 0° for 0, 0.5, 1, 2, 3, 4, and 5 min, respectively). This suggests that a small amount of adsorbed molecules on the SnO_2:F substrate was removed completely by UV irradiation. The surface of the SnO_2:F substrate was covered by hydrophilic OH groups after irradiation. Consequently, the SnO_2:F substrate was modified to have a patterned surface with hydrophobic regions and superhydrophilic regions.

3.2. Liquid-Phase Crystal Deposition of Anatase TiO_2 Thin Films by Heterogeneous Nucleation. The solution became clouded in about 10 min after the mixing of ammonium hexafluorotitanate solution and boric acid solution. The particles were homogeneously nucleated in the solution and made the solution white. They then gradually precipitated and fell to the bottom of the vessel, so the solution became transparent over a period of hours. Ti ions were consumed for crystallization of TiO_2 particles, thus decreasing the ion concentration in the solution. The supersaturation degree of the solution was sufficiently low to realize slow heterogeneous nucleation without homogeneous nucleation, which forms TiO_2 particles. The silicon rubber sponge sheet was removed from the SnO_2:F substrate after 25 h, and the substrate was kept for a further 2 h at 50 °C. Consequently, the patterned surface on the SnO_2:F substrate was exposed to the transparent solution including Ti ions at a low concentration for 2 h. Heterogeneous nucleation and slow crystallization of TiO_2 progressed only on the substrate.

Deposition of anatase TiO_2 proceeds by the following mechanisms[22]

$$TiF_6^{2-} + 2H_2O \leftrightarrows TiO_2 + 4H^+ + 6F^- \quad \text{(a)}$$

$$BO_3^{3-} + 4F^- + 6H^+ \rightarrow BF_4^- + 3H_2O \quad \text{(b)}$$

Equation a is described in detail by the following two equations

$$TiF_6^{2-} \xrightarrow{n\text{OH}^-} TiF_{6-n}(OH)_n^{2-} + nF^- \xrightarrow{(6-n)\text{OH}^-} Ti(OH)_6^{2-} + 6F^- \quad \text{(c)}$$

$$Ti(OH)_6^{2-} \rightarrow TiO_2 + 2H_2O + 2OH^- \quad \text{(d)}$$

Fluorinated titanium complex ions gradually change into titanium hydroxide complex ions in an aqueous solution as shown in eq c. The increase in F^- concentration displaces eqs a and c to the left; however, the produced F^- can be scavenged by H_3BO_3 (BO_3^{3-}), as shown in eq b to displace eqs a and c to the right. Anatase TiO_2 formed from titanium hydroxide complex ions ($Ti(OH)_6^{2-}$) in eq d.

3.3. Change in Solution and Predominant Nucleation. Liquid-phase patterning was not realized in the initial solution but realized in the solution after 25 h. Solution condition was evaluated as a function of time to clarify this reason. The solution was transparent immediately after the mixing of ammonium hexafluorotitanate solution and boric acid solution, became clouded after 0.5 h, and showed maximum whiteness after 1 h (Figure 2a). Anatase TiO_2 particles nucleated homogeneously in the solution and grew to form large particles, which gradually precipitated and made the bottom of the vessel white. The solution became slightly white after 5 h and transparent after 25 h (Figure

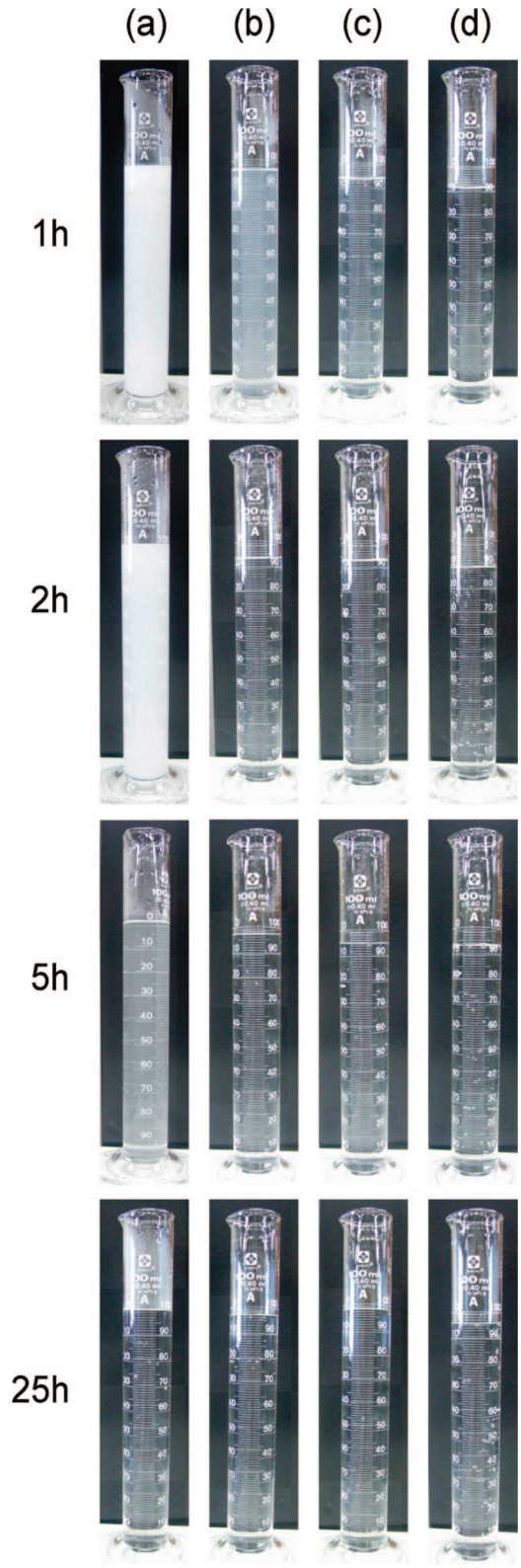

Figure 2. Photographs of supernatant solutions as a function of time before and after filtration. (a) The solution before filtration contains all sizes of suspended particles. (b) The solution filtered by a filter paper (Whatman 5) contains particles <2.5 μm. (c) The solution filtered by a glass filter paper (Whatman GF/B) contains particles <1.0 μm. (d) The solution filtered by a filter syringe (Whatman PTFE 0.2) contains particles <0.2 μm.

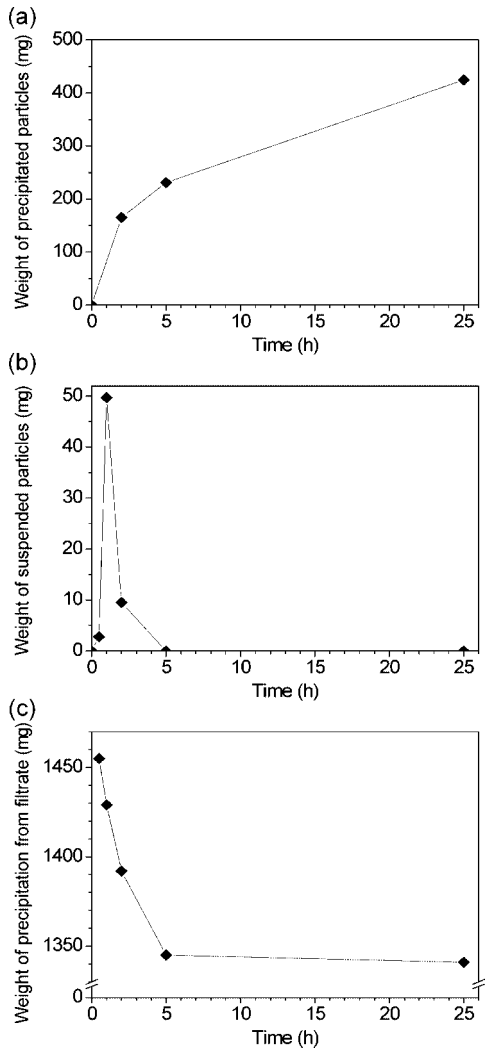

Figure 3. (a) Weight of precipitated particles >2.5 μm as a function of time. (b) Weight of suspended particles >2.5 μm in the supernatant solution as a function of time. (c) Weight of precipitation from filtrate that accumulated in all of the filters.

2a). The solutions changed to transparent by the filtrations (Figure 2). Precipitated particles from the residual solution and particles from the supernatant solution trapped by filters were determined by XRD evaluation to be a single phase of anatase TiO_2.

Precipitated particles from the residual solution increased as 0, 165.1, 230.9, and 424.4 mg at 0, 2, 5, and 25 h, respectively (Figure 3a). The precipitation increased rapidly at the initial stage and moderately after 2 h, reflecting the decrease in crystal growth rate.

The weight of particles >2.5 μm in diameter was estimated to be 2.8, 49.7, 9.5, 0, and 0 mg at 0.5, 1, 2, 5, and 25 h, respectively (Figure 3b). Particles were formed at the initial stage and precipitated, making the bottom of the vessel white. This is consistent with the color change of the solution (Figure 2a).

The precipitate from the filtrate collected by all of the filters was evaluated by XRD. The white powder contained anatase TiO_2, rutile TiO_2, and a large amount of boric acid. These were crystallized from ions in the filtrate during drying. The weight was estimated to be 1455, 1429, 1392, 1345, and 1341 mg at 0.5, 1, 2, 5, and 25 h, respectively (Figure 3c). This indicated that the solution contained a high concentration of ions at the initial stage, which then decreased as a function of time. Ion concentration would decrease by the crystallization and precipitation of anatase TiO_2. This result is consistent with the weight variation of precipitated particles (Figure 3a), weight variation of suspended particles (Figure 3b), and solution color change shown in the photographs (Figure 2a).

Liquid-phase patterning was not realized in the initial clouded solution but realized in the transparent solution after 25 h. Evaluation of solution condition as function of time showed the reason of this phenomenon. TiO_2 particles formed at the initial stage around 1 h and precipitated gradually. Ions were consumed for crystallization of TiO_2 and decreased as a function of time. Heterogeneous nucleation predominantly progressed after 5 h. Consequently, TiO_2 was formed on super hydrophilic regions selectively to realize liquid-phase patterning.

3.4. TEM Observation of Well-Grown Anatase TiO_2 Films. FTO substrate was immersed in the solution for 25 h to form a thick film and ultrasonicated in water for 20 min. The TiO_2 film was constructed of two layers (Figure 4 a). The under layer with a 200 nm thickness was a polycrystalline film of anatase TiO_2. The upper layer with a 300 nm thickness was an assembly of acicular TiO_2 crystals that grew perpendicular to the substrate. The film was shown by electron diffraction pattern to be a single phase of anatase TiO_2 (Figure 4b). Electron diffraction from the 004 plane was stronger than that of the 101, 200, and 211 planes, etc., to show anisotropic crystal growth along the *c*-axis. Additionally, 004 diffractions were strong perpendicular to the substrate, showing that the *c*-axis orientation of acicular crystals was perpendicular to the substrate. The FTO layer was shown to be a single phase of SnO_2 with high crystallinity (Figure 4c). Acicular TiO_2 crystals had a long shape, ~300 nm in length and 10–100 nm in diameter (Figure 4d). A lattice image of anatase TiO_2 was observed from the crystals (Figure 4e).

3.5. Crystal Phase of As-Deposited Films. The film deposited on the substrate was evaluated by XRD analysis. Strong X-ray diffractions were observed for films deposited on FTO substrates and assigned to SnO_2 of FTO films. The 004 diffraction peak of anatase TiO_2 was not observed clearly for TiO_2 film on FTO substrates because both of the weak 004 diffraction peak of TiO_2 and the strong diffraction peak of FTO were observed at the same angle. Glass substrates with no FTO coating were immersed in the solution. Weak X-ray diffraction peaks were observed at $2\theta = 25.3$, 37.7, 48.0, 53.9, 55.1, and 62.7° for the films deposited on glass substrates. They were assigned to 101, 004, 200, 105, 211, and 204 diffraction peaks of anatase TiO_2 (ICSD 9852) (Figure 5). A broad diffraction peak from the glass substrate was also observed at about $2\theta = 25°$.

The intensity of the 004 diffraction peak was stronger than that of the 101 diffraction peak for the film obtained by the liquid-phase crystal deposition method, though the intensity of 101 was stronger than that of 004 for anatase TiO_2 powders with no orientation (ICSD 9852). The integral intensity or peak height of 004 was 2.6 times or 2.2 times

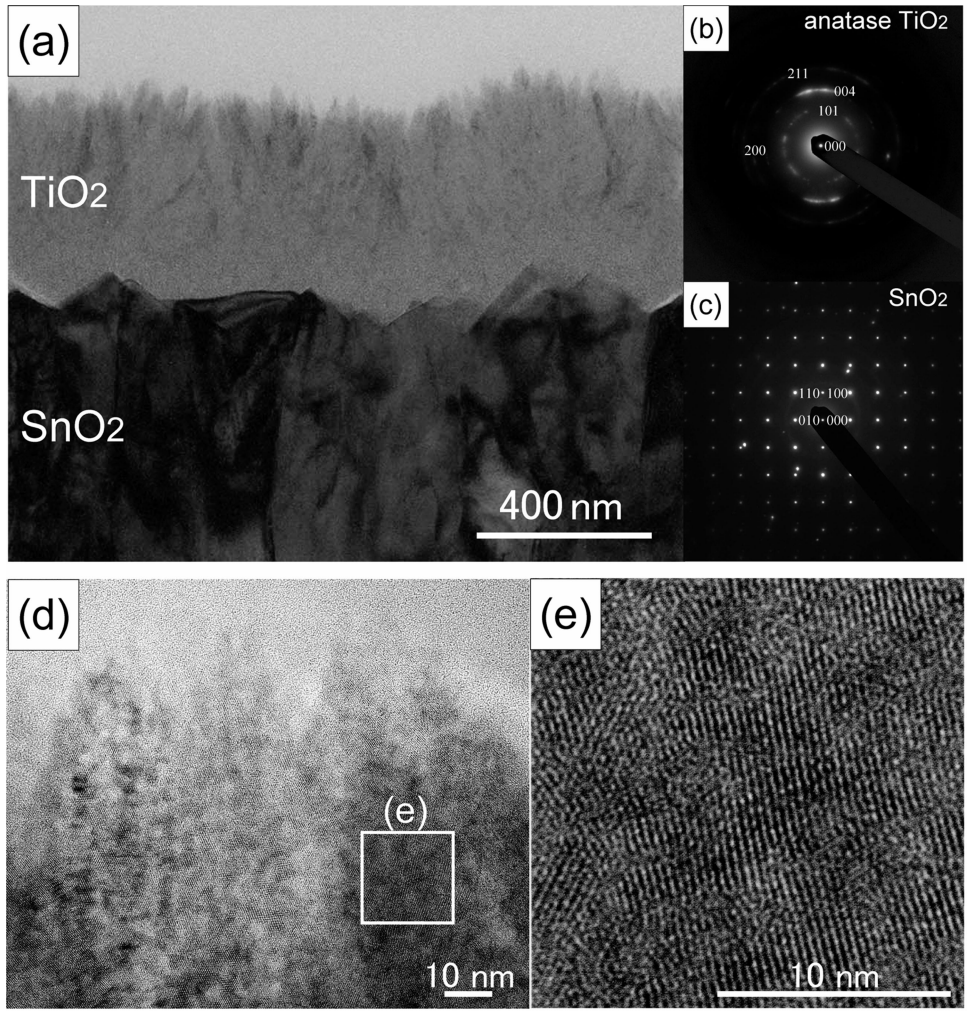

Figure 4. (a) TEM micrograph of anatase TiO_2 film on SnO_2:F substrate. (b) Electron diffraction pattern of anatase TiO_2. (c) Electron diffraction pattern of SnO_2 film. (d) Magnified area of (a) showing morphology of TiO_2 crystals. (e) Magnified area of (d) showing lattice image of TiO_2 crystals.

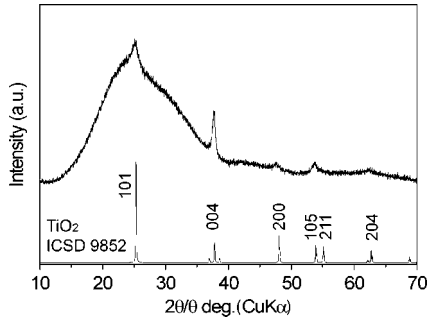

Figure 5. XRD diffraction pattern of anatase TiO_2 film on a glass substrate.

that of 101, respectively, suggesting high *c*-axis orientation of anatase TiO_2 crystals. Crystallite size perpendicular to the 101 or 004 planes was estimated from the full-width half-maximum of the 101 or 004 peak to be 9 or 17 nm, respectively. Elongation of crystals in the *c*-axis direction was also suggested by the difference of crystallite size. These evaluations were consistent with high *c*-axis orientation observed by TEM and electron diffraction. Crystallite size estimated by XRD was similar to that in TiO_2 under layer rather than that of acicular crystals observed by TEM. A TiO_2 thin film prepared on a glass was constructed of not acicular crystals but polycrystals in the bottom layer.

3.6. Liquid-Phase Patterning of Anatase TiO_2 Thin Films. After having been immersed in the solution, the substrate was rinsed with distilled water and dried in air (Figure 1). The initial FTO surface appeared to be blue-green under white light because of the light diffracted from the FTO layer. On the other hand, TiO_2 films deposited on the superhydrophilic surface appeared to be yellow-green. The color change was caused by deposition of a transparent TiO_2 film, which influenced the wavelength of the diffracted light.

The micropattern of TiO_2 was shown by SEM evaluation to be successfully fabricated (Figure 6). TiO_2 deposited on superhydrophilic regions showed black contrast, whereas the initial FTO regions without deposition showed white contrast in Figure 6. The average line width in Figure 6 is 55 μm. Line edge roughness,[44] as measured by the standard deviation of the line width, is $\sim$2.8 μm. This represents $\sim$5% variation (i.e., 2.8/55) in the nominal line width, similar to the usual 5% variation afforded by current electronics design rules. The minimum line width of the pattern depends on the resolution of the photomask and wavelength of irradiated

(44) Masuda, Y.; Sugiyama, T.; Lin, H.; Seo, W. S.; Koumoto, K. *Thin Solid Films* **2001**, *382*, 153–157.

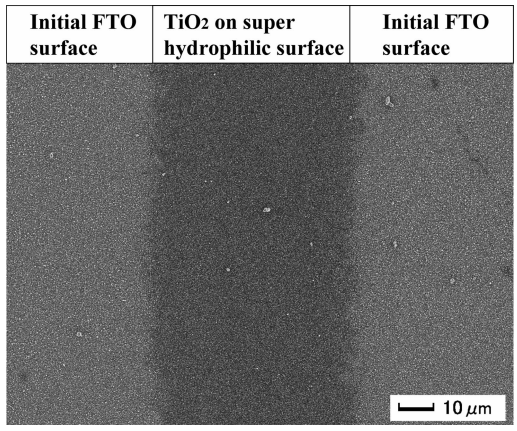

Figure 6. SEM micrograph of a micropattern of anatase TiO_2 films on SnO_2:F substrates.

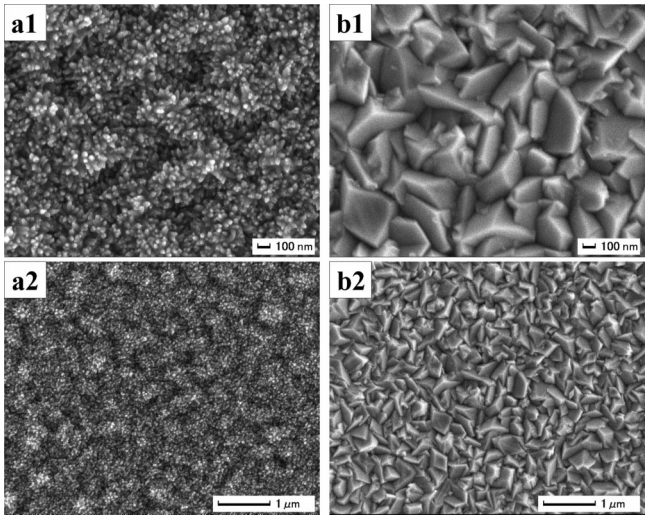

Figure 7. SEM micrographs of a micropattern of anatase TiO_2 films and SnO_2:F substrates. All SEM micrographs are the magnified area of Figure 6. (a1) Surface of anatase TiO_2 films deposited on a superhydrophilic region. TiO_2 was formed on the superhydrophilic region, which was cleaned by UV irradiation before the immersion. (a2) Magnified area of (a1) showing surface morphology of anatase TiO_2 film. (b1) Surface of SnO_2:F substrate without TiO_2 deposition. TiO_2 was not formed on the noncleaned region. (b2) Magnified area of (b1) showing the surface morphology of the SnO_2:F substrate.

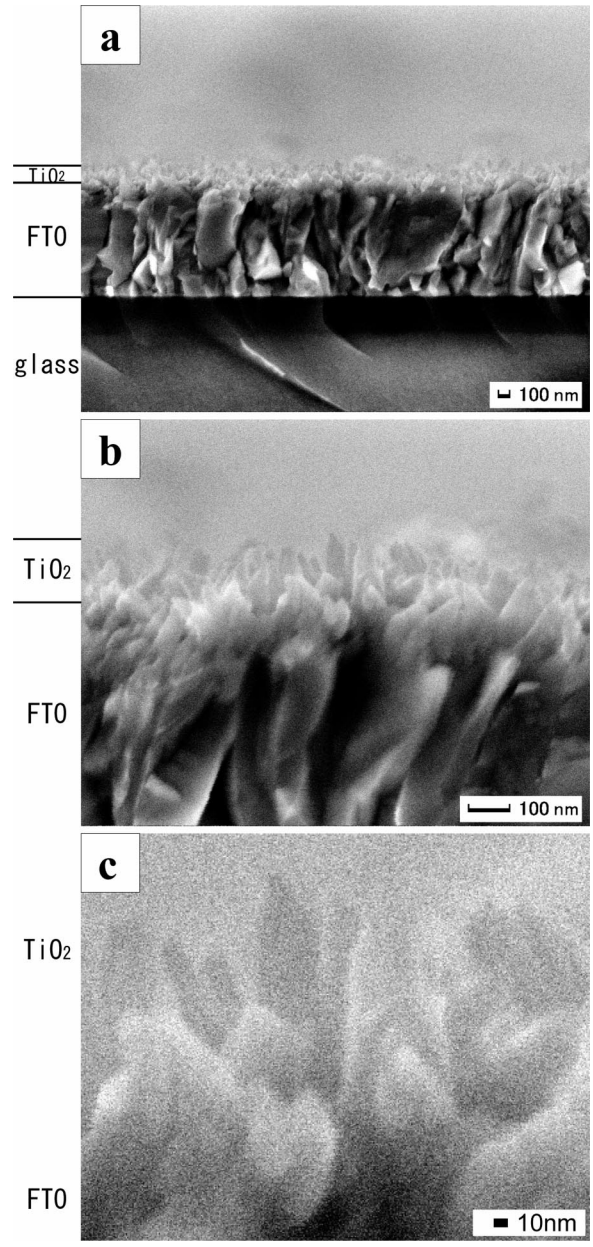

Figure 8. SEM micrographs of anatase TiO_2 films on SnO_2:F substrates. (a) Fracture cross section of TiO_2 films. (b,c) Magnified area of (a) showing morphology of nano TiO_2 crystals.

light (184.9 nm). It was improved to ~1 μm by using a high-resolution photomask.

The FTO layer was a particulate film having a rough surface (images b1 and b2 in Figure 7). Edged particles 100–500 nm in diameter were observed on the surface. The micropattern of TiO_2 thin film was covered by an assembly of nano crystals 10–30 nm in diameter (images a1 and a2 in Figure 7). The nanocrystals were anatase TiO_2 that grew anisotropically. The TiO_2 film also had a large structural relief 100–500 nm in diameter. As the thin TiO_2 film was deposited on the edged particulate surface of the FTO layer, the surface of TiO_2 had a large structural relief.

The morphology of the TiO_2 layer and FTO layer was further observed by fracture cross-section profiles (Figure 8). The polycrystalline FTO layer prepared on a flat glass substrate was shown to have a thickness of ~900 nm and a high roughness of 100–200 nm on the surface (Figure 8a). Nano TiO_2 crystals were deposited on the superhydrophilic FTO surface (Figure 8a), whereas no deposition was observed on the initial FTO surface. The superhydrophilic FTO surface was covered with an array of nano TiO_2 crystals (images b and c in Figure 8), which had a long shape ~150 nm in length and ~20 nm in diameter. These observations were consistent with TEM and XRD evaluations. Nano TiO_2 crystals would grow along the *c*-axis and thus enhance the 004 X-ray diffraction peak and 004 electron diffraction peak. They formed a long shape having a high aspect ratio of 7.5 (150 nm in length/20 nm in diameter) as shown in the SEM fracture cross section profile (images b and c in Figure 8) and TEM micrograph. The orientation of nano TiO_2 crystals with their long axis perpendicular to the FTO layer (Figure 8b, c) would also enhance the 004 diffraction peak.

4. Conclusion

A micropattern of anatase TiO_2 thin film was successfully fabricated on a SnO_2:F substrate in an aqueous solution. Crystalline anatase TiO_2 was deposited by liquid-phase crystal deposition at 50 °C. Nucleation and crystal growth of TiO_2 were accelerated on the superhydrophilic SnO_2:F surface but were suppressed on the hydrophobic initial SnO_2:F surface. Consequently, liquid-phase patterning of anatase TiO_2 was achieved on a SnO_2:F substrate. TiO_2 crystals were directly deposited on the SnO_2:F surface without any insulating layers, which decrease the electrical conductivity between TiO_2 and the SnO_2:F substrate. The micropattern of anatase TiO_2 on the SnO_2:F substrates could be applied to electrodes of dye-sensitized solar cells or molecular sensors. Additionally, this process can be used to form a flexible micropattern of anatase TiO_2 electrodes on low-heat-resistant conductive polymer films. This process will contribute to the microfabrication of TiO_2 electrodes for dye-sensitized solar cells or molecular sensors.

CM071026T